

Production of χ_{c1} and χ_{c2} in $p\bar{p}$ Collisions at $\sqrt{s} = 1.8$ TeV

T. Affolder,²³ H. Akimoto,⁴⁵ A. Akopian,³⁸ M. G. Albrow,¹¹ P. Amaral,⁸ S. R. Amendolia,³⁴
D. Amidei,²⁶ K. Anikeev,²⁴ J. Antos,¹ G. Apollinari,¹¹ T. Arisawa,⁴⁵ T. Asakawa,⁴³
W. Ashmanskas,⁸ F. Azfar,³¹ P. Azzi-Bacchetta,³² N. Bacchetta,³² M. W. Bailey,²⁸
S. Bailey,¹⁶ P. de Barbaro,³⁷ A. Barbaro-Galtieri,²³ V. E. Barnes,³⁶ B. A. Barnett,¹⁹
S. Baroiant,⁵ M. Barone,¹³ G. Bauer,²⁴ F. Bedeschi,³⁴ S. Belforte,⁴² W. H. Bell,¹⁵
G. Bellettini,³⁴ J. Bellinger,⁴⁶ D. Benjamin,¹⁰ J. Bensinger,⁴ A. Beretvas,¹¹ J. P. Berge,¹¹
J. Berryhill,⁸ B. Bevensee,³³ A. Bhatti,³⁸ M. Binkley,¹¹ D. Bisello,³² M. Bishai,¹¹
R. E. Blair,² C. Blocker,⁴ K. Bloom,²⁶ B. Blumenfeld,¹⁹ S. R. Blusk,³⁷ A. Bocci,³⁴
A. Bodek,³⁷ W. Bokhari,³³ G. Bolla,³⁶ Y. Bonushkin,⁶ D. Bortoletto,³⁶ J. Boudreau,³⁵
A. Brandl,²⁸ S. van den Brink,¹⁹ C. Bromberg,²⁷ M. Brozovic,¹⁰ N. Bruner,²⁸ E. Buckley-
Geer,¹¹ J. Budagov,⁹ H. S. Budd,³⁷ K. Burkett,¹⁶ G. Busetto,³² A. Byon-Wagner,¹¹
K. L. Byrum,² P. Calafiura,²³ M. Campbell,²⁶ W. Carithers,²³ J. Carlson,²⁶ D. Carlsmith,⁴⁶
W. Caskey,⁵ J. Cassada,³⁷ A. Castro,³² D. Cauz,⁴² A. Cerri,³⁴ A. W. Chan,¹ P. S. Chang,¹
P. T. Chang,¹ J. Chapman,²⁶ C. Chen,³³ Y. C. Chen,¹ M. -T. Cheng,¹ M. Chertok,⁴⁰

G. Chiarelli,³⁴ I. Chirikov-Zorin,⁹ G. Chlachidze,⁹ F. Chlebana,¹¹ L. Christofek,¹⁸ M. L. Chu,¹
Y. S. Chung,³⁷ C. I. Ciobanu,²⁹ A. G. Clark,¹⁴ A. Connolly,²³ J. Conway,³⁹ M. Cordelli,¹³
J. Cranshaw,⁴¹ D. Cronin-Hennessy,¹⁰ R. Cropp,²⁵ R. Culbertson,¹¹ D. Dagenhart,⁴⁴
S. D'Auria,¹⁵ F. DeJongh,¹¹ S. Dell'Agnello,¹³ M. Dell'Orso,³⁴ L. Demortier,³⁸ M. Deninno,³
P. F. Derwent,¹¹ T. Devlin,³⁹ J. R. Dittmann,¹¹ S. Donati,³⁴ J. Done,⁴⁰ T. Dorigo,¹⁶
N. Eddy,¹⁸ K. Einsweiler,²³ J. E. Elias,¹¹ E. Engels, Jr.,³⁵ R. Erbacher,¹¹ D. Errede,¹⁸
S. Errede,¹⁸ Q. Fan,³⁷ R. G. Feild,⁴⁷ J. P. Fernandez,¹¹ C. Ferretti,³⁴ R. D. Field,¹² I. Fiori,³
B. Flaughner,¹¹ G. W. Foster,¹¹ M. Franklin,¹⁶ J. Freeman,¹¹ J. Friedman,²⁴ Y. Fukui,²²
I. Furic,²⁴ S. Galeotti,³⁴ M. Gallinaro,³⁸ T. Gao,³³ M. Garcia-Sciveres,²³ A. F. Garfinkel,³⁶
P. Gatti,³² C. Gay,⁴⁷ D. W. Gerdes,²⁶ P. Giannetti,³⁴ P. Giromini,¹³ V. Glagolev,⁹
D. Glenzinski,¹¹ M. Gold,²⁸ J. Goldstein,¹¹ A. Gordon,¹⁶ I. Gorelov,²⁸ A. T. Goshaw,¹⁰
Y. Gotra,³⁵ K. Goulianos,³⁸ C. Green,³⁶ G. Grim,⁵ P. Gris,¹¹ L. Groer,³⁹ C. Grosso-
Pilcher,⁸ M. Guenther,³⁶ G. Guillian,²⁶ J. Guimaraes da Costa,¹⁶ R. M. Haas,¹² C. Haber,²³
E. Hafen,²⁴ S. R. Hahn,¹¹ C. Hall,¹⁶ T. Handa,¹⁷ R. Handler,⁴⁶ W. Hao,⁴¹ F. Happacher,¹³
K. Hara,⁴³ A. D. Hardman,³⁶ R. M. Harris,¹¹ F. Hartmann,²⁰ K. Hatakeyama,³⁸ J. Hauser,⁶
J. Heinrich,³³ A. Heiss,²⁰ M. Herndon,¹⁹ C. Hill,⁵ K. D. Hoffman,³⁶ C. Holck,³³ R. Hollebeek,³³
L. Holloway,¹⁸ R. Hughes,²⁹ J. Huston,²⁷ J. Huth,¹⁶ H. Ikeda,⁴³ J. Incandela,¹¹ G. Introzzi,³⁴
J. Iwai,⁴⁵ Y. Iwata,¹⁷ E. James,²⁶ H. Jensen,¹¹ M. Jones,³³ U. Joshi,¹¹ H. Kambara,¹⁴
T. Kamon,⁴⁰ T. Kaneko,⁴³ K. Karr,⁴⁴ H. Kasha,⁴⁷ Y. Kato,³⁰ T. A. Keaffaber,³⁶ K. Kelley,²⁴
M. Kelly,²⁶ R. D. Kennedy,¹¹ R. Kephart,¹¹ D. Khazins,¹⁰ T. Kikuchi,⁴³ B. Kilminster,³⁷

B. J. Kim,²¹ D. H. Kim,²¹ H. S. Kim,¹⁸ M. J. Kim,²¹ S. H. Kim,⁴³ Y. K. Kim,²³ M. Kirby,¹⁰
M. Kirk,⁴ L. Kirsch,⁴ S. Klimenko,¹² P. Koehn,²⁹ A. Königeter,²⁰ K. Kondo,⁴⁵ J. Konigsberg,¹²
K. Kordas,²⁵ A. Korn,²⁴ A. Korytov,¹² E. Kovacs,² J. Kroll,³³ M. Kruse,³⁷ S. E. Kuhlmann,²
K. Kurino,¹⁷ T. Kuwabara,⁴³ A. T. Laasanen,³⁶ N. Lai,⁸ S. Lami,³⁸ S. Lammel,¹¹
J. I. Lamoureux,⁴ J. Lancaster,¹⁰ M. Lancaster,²³ R. Lander,⁵ G. Latino,³⁴ T. LeCompte,²
A. M. Lee IV,¹⁰ K. Lee,⁴¹ S. Leone,³⁴ J. D. Lewis,¹¹ M. Lindgren,⁶ T. M. Liss,¹⁸ J. B. Liu,³⁷
Y. C. Liu,¹ N. Lockyer,³³ J. Loken,³¹ M. Loreti,³² D. Lucchesi,³² P. Lukens,¹¹ S. Lusin,⁴⁶
L. Lyons,³¹ J. Lys,²³ R. Madrak,¹⁶ K. Maeshima,¹¹ P. Maksimovic,¹⁶ L. Malferrari,³
M. Mangano,³⁴ M. Mariotti,³² G. Martignon,³² A. Martin,⁴⁷ J. A. J. Matthews,²⁸ J. Mayer,²⁵
P. Mazzanti,³ K. S. McFarland,³⁷ P. McIntyre,⁴⁰ E. McKigney,³³ M. Menguzzato,³²
A. Menzione,³⁴ C. Mesropian,³⁸ A. Meyer,¹¹ T. Miao,¹¹ R. Miller,²⁷ J. S. Miller,²⁶
H. Minato,⁴³ S. Miscetti,¹³ M. Mishina,²² G. Mitselmakher,¹² N. Moggi,³ E. Moore,²⁸
R. Moore,²⁶ Y. Morita,²² T. Moulik,²⁴ M. Mulhearn,²⁴ A. Mukherjee,¹¹ T. Muller,²⁰
A. Munar,³⁴ P. Murat,¹¹ S. Murgia,²⁷ J. Nachtman,⁶ S. Nahn,⁴⁷ H. Nakada,⁴³ T. Nakaya,⁸
I. Nakano,¹⁷ C. Nelson,¹¹ T. Nelson,¹¹ C. Neu,²⁹ D. Neuberger,²⁰ C. Newman-Holmes,¹¹
C.-Y. P. Ngan,²⁴ H. Niu,⁴ L. Nodulman,² A. Nomerotski,¹² S. H. Oh,¹⁰ T. Ohmoto,¹⁷
T. Ohsugi,¹⁷ R. Oishi,⁴³ T. Okusawa,³⁰ J. Olsen,⁴⁶ W. Orejudos,²³ C. Pagliarone,³⁴
F. Palmonari,³⁴ R. Paoletti,³⁴ V. Papadimitriou,⁴¹ S. P. Pappas,⁴⁷ D. Partos,⁴ J. Patrick,¹¹
G. Pauletta,⁴² M. Paulini,^{(*) 23} C. Paus,²⁴ L. Pescara,³² T. J. Phillips,¹⁰ G. Piacentino,³⁴
K. T. Pitts,¹⁸ A. Pompos,³⁶ L. Pondrom,⁴⁶ G. Pope,³⁵ M. Popovic,²⁵ F. Prokoshin,⁹

J. Proudfoot,² F. Ptohos,¹³ O. Pukhov,⁹ G. Punzi,³⁴ K. Ragan,²⁵ A. Rakitine,²⁴ D. Reher,²³
A. Reichold,³¹ A. Ribon,³² W. Riegler,¹⁶ F. Rimondi,³ L. Ristori,³⁴ M. Riveline,²⁵
W. J. Robertson,¹⁰ A. Robinson,²⁵ T. Rodrigo,⁷ S. Rolli,⁴⁴ L. Rosenson,²⁴ R. Roser,¹¹
R. Rossin,³² A. Roy,²⁴ A. Safonov,³⁸ R. St. Denis,¹⁵ W. K. Sakumoto,³⁷ D. Saltzberg,⁶
C. Sanchez,²⁹ A. Sansoni,¹³ L. Santi,⁴² H. Sato,⁴³ P. Savard,²⁵ P. Schlabach,¹¹ E. E. Schmidt,¹¹
M. P. Schmidt,⁴⁷ M. Schmitt,¹⁶ L. Scodellaro,³² A. Scott,⁶ A. Scribano,³⁴ S. Segler,¹¹
S. Seidel,²⁸ Y. Seiya,⁴³ A. Semenov,⁹ F. Semeria,³ T. Shah,²⁴ M. D. Shapiro,²³ P. F. Shepard,³⁵
T. Shibayama,⁴³ M. Shimojima,⁴³ M. Shochet,⁸ J. Siegrist,²³ G. Signorelli,³⁴ A. Sill,⁴¹
P. Sinervo,²⁵ P. Singh,¹⁸ A. J. Slaughter,⁴⁷ K. Sliwa,⁴⁴ C. Smith,¹⁹ F. D. Snider,¹¹
A. Solodsky,³⁸ J. Spalding,¹¹ T. Speer,¹⁴ P. Sphicas,²⁴ F. Spinella,³⁴ M. Spiropulu,¹⁶
L. Spiegel,¹¹ J. Steele,⁴⁶ A. Stefanini,³⁴ J. Strologas,¹⁸ F. Strumia,¹⁴ D. Stuart,¹¹
K. Sumorok,²⁴ T. Suzuki,⁴³ T. Takano,³⁰ R. Takashima,¹⁷ K. Takikawa,⁴³ P. Tamburello,¹⁰
M. Tanaka,⁴³ B. Tannenbaum,⁶ W. Taylor,²⁵ M. Tecchio,²⁶ R. Tesarek,¹¹ P. K. Teng,¹
K. Terashi,³⁸ S. Tether,²⁴ A. S. Thompson,¹⁵ R. Thurman-Keup,² P. Tipton,³⁷ S. Tkaczyk,¹¹
K. Tollefson,³⁷ A. Tollestrup,¹¹ H. Toyoda,³⁰ W. Trischuk,²⁵ J. F. de Troconiz,¹⁶ J. Tseng,²⁴
N. Turini,³⁴ F. Ukegawa,⁴³ T. Vaiciulis,³⁷ J. Valls,³⁹ S. Vejcik III,¹¹ G. Velev,¹¹ R. Vidal,¹¹
R. Vilar,⁷ I. Volobouev,²³ D. Vucinic,²⁴ R. G. Wagner,² R. L. Wagner,¹¹ J. Wahl,⁸
N. B. Wallace,³⁹ A. M. Walsh,³⁹ C. Wang,¹⁰ M. J. Wang,¹ T. Watanabe,⁴³ D. Waters,³¹
T. Watts,³⁹ R. Webb,⁴⁰ H. Wenzel,²⁰ W. C. Wester III,¹¹ A. B. Wicklund,² E. Wicklund,¹¹
T. Wilkes,⁵ H. H. Williams,³³ P. Wilson,¹¹ B. L. Winer,²⁹ D. Winn,²⁶ S. Wolbers,¹¹

D. Wolinski,²⁶ J. Wolinski,²⁷ S. Wolinski,²⁶ S. Worm,²⁸ X. Wu,¹⁴ J. Wyss,³⁴ A. Yagil,¹¹
W. Yao,²³ G. P. Yeh,¹¹ P. Yeh,¹ J. Yoh,¹¹ C. Yosef,²⁷ T. Yoshida,³⁰ I. Yu,²¹ S. Yu,³³ Z. Yu,⁴⁷
A. Zanetti,⁴² F. Zetti,²³ and S. Zucchelli³

(CDF Collaboration)

¹ *Institute of Physics, Academia Sinica, Taipei, Taiwan 11529, Republic of China*

² *Argonne National Laboratory, Argonne, Illinois 60439*

³ *Istituto Nazionale di Fisica Nucleare, University of Bologna, I-40127 Bologna, Italy*

⁴ *Brandeis University, Waltham, Massachusetts 02254*

⁵ *University of California at Davis, Davis, California 95616*

⁶ *University of California at Los Angeles, Los Angeles, California 90024*

⁷ *Instituto de Fisica de Cantabria, CSIC-University of Cantabria, 39005 Santander, Spain*

⁸ *Enrico Fermi Institute, University of Chicago, Chicago, Illinois 60637*

⁹ *Joint Institute for Nuclear Research, RU-141980 Dubna, Russia*

¹⁰ *Duke University, Durham, North Carolina 27708*

¹¹ *Fermi National Accelerator Laboratory, Batavia, Illinois 60510*

¹² *University of Florida, Gainesville, Florida 32611*

¹³ *Laboratori Nazionali di Frascati, Istituto Nazionale di Fisica Nucleare, I-00044 Frascati, Italy*

¹⁴ *University of Geneva, CH-1211 Geneva 4, Switzerland*

¹⁵ *Glasgow University, Glasgow G12 8QQ, United Kingdom*

- ¹⁶ *Harvard University, Cambridge, Massachusetts 02138*
- ¹⁷ *Hiroshima University, Higashi-Hiroshima 724, Japan*
- ¹⁸ *University of Illinois, Urbana, Illinois 61801*
- ¹⁹ *The Johns Hopkins University, Baltimore, Maryland 21218*
- ²⁰ *Institut für Experimentelle Kernphysik, Universität Karlsruhe, 76128 Karlsruhe, Germany*
- ²¹ *Center for High Energy Physics: Kyungpook National University, Taegu 702-701; Seoul National University, Seoul 151-742; and SungKyunKwan University, Suwon 440-746; Korea*
- ²² *High Energy Accelerator Research Organization (KEK), Tsukuba, Ibaraki 305, Japan*
- ²³ *Ernest Orlando Lawrence Berkeley National Laboratory, Berkeley, California 94720*
- ²⁴ *Massachusetts Institute of Technology, Cambridge, Massachusetts 02139*
- ²⁵ *Institute of Particle Physics: McGill University, Montreal H3A 2T8; and University of Toronto, Toronto M5S 1A7;*
Canada
- ²⁶ *University of Michigan, Ann Arbor, Michigan 48109*
- ²⁷ *Michigan State University, East Lansing, Michigan 48824*
- ²⁸ *University of New Mexico, Albuquerque, New Mexico 87131*
- ²⁹ *The Ohio State University, Columbus, Ohio 43210*
- ³⁰ *Osaka City University, Osaka 588, Japan*
- ³¹ *University of Oxford, Oxford OX1 3RH, United Kingdom*
- ³² *Università di Padova, Istituto Nazionale di Fisica Nucleare, Sezione di Padova, I-35131 Padova, Italy*
- ³³ *University of Pennsylvania, Philadelphia, Pennsylvania 19104*

³⁴ *Istituto Nazionale di Fisica Nucleare, University and Scuola Normale Superiore of Pisa, I-56100 Pisa, Italy*

³⁵ *University of Pittsburgh, Pittsburgh, Pennsylvania 15260*

³⁶ *Purdue University, West Lafayette, Indiana 47907*

³⁷ *University of Rochester, Rochester, New York 14627*

³⁸ *Rockefeller University, New York, New York 10021*

³⁹ *Rutgers University, Piscataway, New Jersey 08855*

⁴⁰ *Texas A&M University, College Station, Texas 77843*

⁴¹ *Texas Tech University, Lubbock, Texas 79409*

⁴² *Istituto Nazionale di Fisica Nucleare, University of Trieste/ Udine, Italy*

⁴³ *University of Tsukuba, Tsukuba, Ibaraki 305, Japan*

⁴⁴ *Tufts University, Medford, Massachusetts 02155*

⁴⁵ *Waseda University, Tokyo 169, Japan*

⁴⁶ *University of Wisconsin, Madison, Wisconsin 53706*

⁴⁷ *Yale University, New Haven, Connecticut 06520*

(*) *Now at Carnegie Mellon University, Pittsburgh, Pennsylvania 15213*

Abstract

We have measured the ratio of prompt production rates of the charmonium states χ_{c1} and χ_{c2} in 110 pb^{-1} of $p\bar{p}$ collisions at $\sqrt{s} = 1.8 \text{ TeV}$. The photon from their decay into $J/\psi\gamma$ is reconstructed through conversion into e^+e^- pairs. The energy resolution this technique provides makes the resolution of the two states possible. We find the ratio of production cross sections $\frac{\sigma_{\chi_{c2}}}{\sigma_{\chi_{c1}}} = 0.96 \pm 0.27(\text{stat.}) \pm 0.11(\text{sys.})$ for events with $p_T(J/\psi) > 4.0 \text{ GeV}/c$, $|\eta(J/\psi)| < 0.6$, and $p_T(\gamma) > 1.0 \text{ GeV}/c$.

The production of charmonium in $p\bar{p}$ collisions occurs promptly, or through the decay of hadrons containing the b quark. Prompt charmonium production can be easily separated from B hadron decay backgrounds using the lifetime distributions. The cross section of prompt J/ψ 's can be described by calculations based on the Nonrelativistic QCD factorization formalism [1, 2] that include both color singlet and color octet contributions [3, 4]. However, these QCD calculations of charmonium production predict a large transverse polarization of the J/ψ and $\psi(2S)$ which is not seen in the data [5]. This discrepancy between the experimental observations and theoretical understanding of prompt charmonium production heightens the importance of exploring such processes as completely as possible.

In this paper, we contribute to the study of the charmonium system by measuring the relative cross sections of the χ_{c1} and χ_{c2} promptly produced in $p\bar{p}$ collisions at $\sqrt{s}=1.8$ TeV using the Collider Detector at Fermilab (CDF). Knowledge of this ratio is needed for any model that calculates J/ψ production through radiative χ_c decay, and can be an important standard for comparing production models. We study the process $p\bar{p} \rightarrow \chi_{cJ}X$, $\chi_{cJ} \rightarrow J/\psi\gamma$, $J/\psi \rightarrow \mu^+\mu^-$, where χ_{cJ} is taken to represent χ_{c1} or χ_{c2} . The final state photons are reconstructed through conversion into e^+e^- pairs, which provide excellent energy resolution for the photons from χ_{cJ} decay. The resulting $J/\psi\gamma$ mass resolution allows us to distinguish the χ_{c1} and χ_{c2} , and thereby perform the measurement. This measurement is based on 110

pb^{-1} of data taken during the 1992-95 operation of the Tevatron.

The CDF detector has been described in detail elsewhere [6]. Charged particles emerging from the $p\bar{p}$ interaction point are detected in a silicon vertex detector (SVX), a time projection chamber (VTX), and a central tracking chamber (CTC). These tracking detectors are located in a 1.4 Tesla solenoidal field. Our coordinate system defines the z axis to be the proton beam direction, with ϕ and r being the azimuthal angle and transverse distance, respectively. The CTC, an 84 layer drift chamber, covers the pseudorapidity interval $|\eta| < 1$ (where $\eta \equiv -\ln(\tan(\theta/2))$ and θ is the angle with respect to the proton beam direction) and provides information in both the $r-z$ and $r-\phi$ views. The efficiency for track reconstruction in the CTC cuts off for tracks with $p_T < 0.2 \text{ GeV}/c$, rises over the range $0.2 \text{ GeV}/c < p_T < 0.4 \text{ GeV}/c$, and reaches $\approx 93\%$ for tracks with $p_T > 0.4 \text{ GeV}/c$, where p_T is the track transverse momentum. The SVX extends over approximately 60% of the interaction region. This detector provides track impact parameter measurements for the muons from J/ψ decay in the $r-\phi$ view with a resolution of $(13 + 40/p_T) \mu\text{m}$, where p_T is in GeV/c . The combined momentum resolution of the tracking chambers is $\delta p_T/p_T = [(0.0009p_T)^2 + (0.0066)^2]^{1/2}$, where p_T is in GeV/c . The beam pipe, SVX, VTX, and inner support cylinder of the CTC contribute to an average thickness of $6.02 \pm 0.33\%$ radiation lengths of material [7], as measured perpendicular to the beamline.

Muons from the decay $J/\psi \rightarrow \mu^+\mu^-$ are identified by drift chambers located outside the electromagnetic and hadron calorimeters. The central muon chambers used in this

analysis cover the region $|\eta| < 0.6$, and are used in a three level trigger system to require a pair of muons in the event. The first trigger level identifies muon candidates by requiring a coincidence between two radially aligned muon chambers. Two such coincidences are required for this trigger. The second dimuon trigger level combines the muon candidates with information from the fast track processor in the CTC. For the first 19.4 pb^{-1} of data collected, a single match between a muon chamber coincidence and a CTC track with $p_T > 2.8 \text{ GeV}/c$ was required. For the remainder of the data, this trigger required two such matches with track $p_T > 2.0 \text{ GeV}/c$. The final level of the trigger was performed in software, and required events to contain oppositely charged muon candidate pairs with an invariant mass within approximately $300 \text{ MeV}/c^2$ of the world average J/ψ mass of $3096.9 \text{ MeV}/c^2$ [8].

The $J/\psi \rightarrow \mu^+\mu^-$ candidates are selected by requiring events that satisfy all trigger requirements after offline reconstruction, and have $p_T(J/\psi) > 4.0 \text{ GeV}/c$. A simultaneous mass and vertex constrained fit is performed on the muon tracks, where the dimuon mass is constrained to the J/ψ mass. We find $\sim 151\,000$ events have a good fit to the J/ψ mass. A subset of $\sim 88\,000$ events have both decay muons measured within the SVX, which provides vertex resolution sufficient for determining the fraction of events due to B hadron decay.

The search for photon conversion candidates begins with a scan of all additional tracks found in each J/ψ event. Pairs of oppositely charged tracks are chosen with $\cos(\theta_{e-e}) > 0.995$, where θ_{e-e} is the opening angle between the tracks at the point of intersection. These

pairs have their track parameters recalculated by using a least squares fit, with constraints consistent with the photon conversion hypothesis. Specifically, the two tracks are constrained to be parallel at their point of intersection, and the momentum of the pair is constrained to pass through the dimuon vertex. The radial distance from the dimuon vertex to the intersection point is required to be 1.0 cm or more in order to reduce the background due to particles originating from the primary vertex. Also, we require $p_T(\gamma) > 1.0 \text{ GeV}/c$ and $p_T(e^\pm) > 0.4 \text{ GeV}/c$. A final fit on all four particle trajectories is then performed that simultaneously constrains the muon momenta to form the world average J/ψ mass [8] and the γ momentum to point to the dimuon vertex.

Relative acceptance and reconstruction efficiencies for $J/\psi\gamma$ final states of different invariant mass have been studied with simulated events generated with a $p_T(\chi_{cJ})$ distribution that was tuned to match the distribution of events seen in the data [4]. Monte Carlo generated $\chi_{cJ} \rightarrow J/\psi\gamma$ events are used as input to the detector and trigger simulations, to provide a measure of our acceptance for the χ_{cJ} states. The larger mass of the χ_{c2} gives a higher efficiency at low $p_T(\chi_{cJ})$ than for the χ_{c1} ; this difference vanishes for $\frac{p_T(\chi_{cJ})}{M(\chi_{cJ})} \gg 1$. The overall efficiency ratio is found to be $\frac{\epsilon_{\chi_{c1}}}{\epsilon_{\chi_{c2}}} = 0.85 \pm 0.014$, where the uncertainty is due to the simulated event sample size and uncertainty in the $p_T(\chi_{cJ})$ distribution used in the simulation.

Systematic effects that might change the reconstruction efficiency ratio $\frac{\epsilon_{\chi_{c1}}}{\epsilon_{\chi_{c2}}}$ would have to affect one spin state differently from the other. The decay angle distribution is one such

possibility, and an estimate of our sensitivity to differences between the two states is made by convoluting a distribution of the form $1 + \alpha_{\mu-\gamma} \cos^2(\theta_{\mu-\gamma})$, where $\alpha_{\mu-\gamma}$ is a constant and $\theta_{\mu-\gamma}$ is the angle between the photon and μ^- measured in the $J/\psi\gamma$ rest frame, with the efficiency distribution. The results of this calculation indicate that values of $\alpha_{\mu-\gamma}$ over the range -1 to $+1$ correspond to a variation in the χ_{cJ} reconstruction efficiency of $\pm 7\%$. We have taken half of this variation as the systematic uncertainty on the relative efficiency ratio $\frac{\epsilon_{\chi_{c1}}}{\epsilon_{\chi_{c2}}}$ due to possible decay angle distributions.

Any differences in the production of the two states associated with the polarization or $p_T(\chi_{cJ})$ distributions would require different production mechanisms for the χ_{c1} and χ_{c2} , and is therefore considered to be unlikely. The data are too sparse to provide much guidance. Therefore, we have assigned no systematic uncertainty on $\frac{\epsilon_{\chi_{c1}}}{\epsilon_{\chi_{c2}}}$ due to possible differences in the χ_{c1} and χ_{c2} production kinematics.

The predominant χ_{cJ} background is due to photons resulting from the decay of π^0, η , and K_s^0 mesons produced in association with the J/ψ . To model this background, charged tracks that originate from the J/ψ vertex in the data are used to define the momentum of simulated π^0, η , and K_s^0 's produced in the ratio 4:2:1 respectively as was done in [4]. The simulated decay of these particles provides a photon spectrum that, taken with the J/ψ , yields a $J/\psi\gamma$ mass spectrum whose shape is used to model the background under the χ_{cJ} states. Our sensitivity to the $\pi^0 : \eta : K_s^0$ ratio is negligible since the background variation is small over the range of $J/\psi\gamma$ mass combinations used in this analysis.

Although the production of $h_c(1P)$ mesons is poorly established [8], we nonetheless consider it a second source of background to the χ_{c1} , due to its mass ($3526 \pm 0.24 \text{ MeV}/c^2$) and the partial reconstruction, $h_c \rightarrow J/\psi\pi^0, \pi^0 \rightarrow \gamma\gamma$. A Monte Carlo simulation of h_c production and decay, along with reconstruction of only one final state photon, provided a $J/\psi\gamma$ mass spectrum for this background component. We find the overall h_c acceptance with respect to the χ_{c1} to be $\frac{\epsilon_{h_c}}{\epsilon_{\chi_{c1}}} = 0.523 \pm 0.005$. The cross sections for h_c and χ_{c1} are predicted to be comparable [10], and the h_c branching ratio to $J/\psi\pi^0$ is predicted to be 0.5 – 1.0% [11]. Taken together, these predictions and our efficiency suggest that the number of h_c events in our data should be 0.01-0.02 times the number of χ_{c1} events.

The decay of hadrons containing b quarks provides another background to prompt χ_{cJ} production. We use the decay length measured in the SVX to discriminate between χ_c events produced promptly and through B decay processes. Since any $J/\psi\gamma$ combination that originates from B decay provides only a partial reconstruction of the B hadron, the proper decay length is not directly measurable. We therefore use the effective decay length $\lambda_{eff} = L_{xy} \frac{M(J/\psi)}{p_T(J/\psi) F_{corr}(p_T(J\psi))}$ where $M(J/\psi)$ and $p_T(J/\psi)$ are the mass and transverse momentum respectively of the J/ψ , L_{xy} is the measured displacement of the dimuon vertex in the direction of its transverse momentum, and $F_{corr}(p_T(J\psi))$ is a correction factor between the B and J/ψ momentum, which is obtained by Monte Carlo simulation of B hadron decay [9].

The $J/\psi\gamma$ mass spectrum is shown in Fig. 1. The χ_{c1} and χ_{c2} are clearly resolved, although no evidence for the χ_{c0} is seen in this distribution. The effective decay length

distribution for events measured in the SVX is shown in Fig. 2. The mass and decay length distributions are fit simultaneously using the maximum likelihood method to obtain the number of χ_{cJ} events due to prompt production. The likelihood function used is given by

$$\mathcal{L} = \prod_{i=1}^N [f_1 F_{\chi_1}^i + f_2 F_{\chi_2}^i + (1 - f_1 - f_2) F_{bck}^i] \quad (1)$$

where f_1, f_2 are the fractions of the events in the χ_{c1}, χ_{c2} signals, $F_{\chi_1}^i, F_{\chi_2}^i$ are the products of the mass and effective decay length distributions for the signals, F_{bck}^i is the product of mass and effective decay length distributions for the background, and N is the total number of events.

The function representing the signal shape consists of two Gaussians whose characteristic width is given by the measured mass uncertainty for each event, times a scale factor. The mass is allowed to vary in the fit, but the difference in mass between the two signals is constrained to the known χ_{c1}/χ_{c2} mass difference of 46 MeV/ c^2 [8]. The background function shape was determined by the Monte Carlo method described above, and its normalization was allowed to vary in the fit.

The decay length distributions used for both signals and the background consist of a sum of prompt and B decay components. The prompt contribution is a Gaussian centered at the beam position, with a characteristic width that is given by the decay length uncertainty calculated for each event. The B decay contribution is a convolution between an exponential distribution with a characteristic decay length and the decay length uncertainty for each event. The relative contribution between the prompt and B decay components is allowed

to vary for each signal and the background independently. The characteristic proper decay length is constrained to $470 \mu\text{m}$, the average decay length for B hadron mixtures [8], for both signals and background. Although all events were subjected to the same likelihood fit, only the events measured in the SVX have the decay length resolution to contribute significantly to separating the prompt and B decay components.

The fit gives 118.7 ± 13.5 total χ_{cJ} events, and a χ_{c1} mass of $3508.3 \pm 0.7 \text{ MeV}/c^2$. The ratio of events between the χ_{c1} and χ_{c2} is measured to be $\frac{N_{\chi_{c2}}}{N_{\chi_{c1}}} = 0.63 \pm 0.15$ for the full data sample, where $N_{\chi_{cJ}}$ is the number of events obtained for each χ_{cJ} . Decays of B hadrons are found to contribute $(8 \pm 5\%)$, $(18 \pm 9\%)$, and $(25 \pm 3\%)$ to the χ_{c1} , χ_{c2} , and background respectively. The ratio of events in the prompt subset of the data is then $\frac{N_{\chi_{c2}}}{N_{\chi_{c1}}} \frac{1-f_{b2}}{1-f_{b1}} = 0.56 \pm 0.16$, where $N_{\chi_{cJ}}$ is the number of events measured, and f_{bJ} are the fractions of events due to B decay. Variation of the characteristic decay length by $\pm 50 \mu\text{m}$ corresponded to a change in the prompt yield ratio of less than 10^{-3} , so no systematic uncertainty has been attributed to the choice of decay length used in the fit. Variation of the h_c contribution to the background by $\pm 0.01 N_{\chi_{c1}}$ produced a $\pm 0.4\%$ change in the measurement of the the prompt event ratio, which is used as a systematic uncertainty.

The ratio of prompt cross sections for the χ_{c1} and χ_{c2} is given by

$$\frac{\sigma_{\chi_{c2}}}{\sigma_{\chi_{c1}}} = \frac{N_{\chi_{c2}}(1-f_{b2})\epsilon_{\chi_{c1}}B(\chi_{c1} \rightarrow J/\psi\gamma)}{N_{\chi_{c1}}(1-f_{b1})\epsilon_{\chi_{c2}}B(\chi_{c2} \rightarrow J/\psi\gamma)} \quad (2)$$

where $\sigma_{\chi_{cJ}}$ is the production cross section, $\epsilon_{\chi_{cJ}}$ is the reconstruction acceptance and efficiency, and $B(\chi_{cJ} \rightarrow J/\psi\gamma)$ is the branching ratio into the $J/\psi\gamma$ final state for each of the χ_{cJ} states.

The ratio of decay branching ratios is $\frac{B(\chi_{c1} \rightarrow J/\psi\gamma)}{B(\chi_{c2} \rightarrow J/\psi\gamma)} = \frac{27.3 \pm 1.6\%}{13.5 \pm 1.1\%} = (2.02 \pm 0.20)$, assuming the two values are uncorrelated [8]. Consequently, we are left with a relative systematic uncertainty on the ratio of cross sections of $\pm 10\%$ due to the branching ratio uncertainties.

Table I: Systematic uncertainties for the relative rate of χ_{cJ} production.

Effect	Uncertainty
Possible h_c background	+0.4%, -0
Efficiency Ratio Uncertainty	$\pm 1.4\%$
Decay Angular Distribution	$\pm 3.5\%$
Branching Ratios	$\pm 10\%$
Total	$\pm 11\%$

The systematic uncertainties for the relative rate of production are summarized in Table I. The individual uncertainties are combined in quadrature to give the total systematic uncertainty on the cross section ratio. Our final result on the relative rate of prompt production is then

$$\frac{\sigma_{\chi_{c2}}}{\sigma_{\chi_{c1}}} = 0.96 \pm 0.27(stat.) \pm 0.11(sys.). \quad (3)$$

Previous measurements of the χ_{c2}/χ_{c1} ratio have been at fixed target experiments [12], operating at lower energies than those obtained at the Tevatron. Despite significant theoretical efforts to understand charmonium production in that environment [13, 14], the comparison between this result and those is not straightforward. The present measurement provides a similar constraint on theoretical understanding of charmonium production at the Tevatron. This result appears to prefer an approximately equal production of the two χ_{cJ} states, although it is consistent with the expectation that the cross sections are proportional to

$(2J + 1)$ at high $p_t(\chi_{cJ})$ [14]. A recent NRQCD prediction for the cross section ratio is 1.1 ± 0.2 [15], in good agreement with this measurement.

We thank the Fermilab staff and the technical staffs of the participating institutions for their vital contributions. This work was supported by the U.S. Department of Energy and National Science Foundation, the Italian Istituto Nazionale di Fisica Nucleare, the Ministry of Education, Science and Culture of Japan, the Natural Sciences and Engineering Research Council of Canada, the National Science Council of the Republic of China, and the A.P. Sloan Foundation.

References

- [1] G.T. Bodwin, E. Braaten, and G. Lepage, Phys. Rev. D **51**, 1125 (1995) (Erratum *ibid.* **55**, 5853(1997)).
- [2] E. Braaten and S. Fleming, Phys. Rev. Lett. **74**, 3327 (1995); P. Cho and A. Leibovich, Phys. Rev. D **53**, 150 (1996); P. Cho and A. Leibovich, Phys. Rev. D **53**, 6203 (1996).
- [3] F. Abe *et al.*, Phys. Rev. Lett. **79**, 572 (1997).
- [4] F. Abe *et al.*, Phys. Rev. Lett. **79**, 578 (1997).
- [5] T. Affolder *et al.*, Phys. Rev. Lett. **85**, 2886 (2000).

- [6] F. Abe *et al.*, Nucl. Instr. Meth. Phys. Res. **271**, 387 (1988); D. Amidei *et al.*, Nucl. Instr. Meth. Phys. Res., Sect. A, **350**, 73 (1994); F. Abe *et al.*, Phys. Rev. D **50**, 2966 (1994).
- [7] F. Abe *et al.*, Phys. Rev. D **52**, 4784 (1995).
- [8] D.E. Groom *et al.*, Eur. Phys. J. **C15**, 1 (2000).
- [9] F. Abe *et al.*, Phys. Rev. D **57**, 5382 (1998).
- [10] K. Sridhar, Phys. Rev. Lett. **77**, 4880 (1996).
- [11] Y.-P. Kuang, S.F. Tuan, and T.-M. Yan, Phys. Rev. D **37**, 1210 (1988).
- [12] Y. Lemoigne *et al.*, Phys. Lett. **113B**, 509 (1982); S. R. Hahn, *et al.*, Phys. Rev. D **30**, 671 (1984); L. Antoniazzi *et al.*, Phys. Rev. Lett. **70**, 383 (1993); L. Antoniazzi *et al.*, Phys. Rev. D **49**, 543 (1994); V. Koreshev *et al.*, Phys. Rev. Lett. **77**, 4294 (1996); T. Alexopoulos *et al.*, Phys. Rev. D **62**, 032006 (2000);
- [13] M. Beneke and I. Z. Rothstein, Phys. Rev. D **54**, 2005 (1996), M. Vanttinen, P. Hoyer, S.J. Brodsky, and W.-K. Tang, Phys. Rev. D **51**, 3332 (1995).
- [14] G. A. Schuler, Z. Phys. **C71**, 317 (1996).
- [15] F. Maltoni, private communication. Work based on [1, 2], and E. Eichten and C. Quigg, Phys. Rev. D **52**, 1726 (1995).

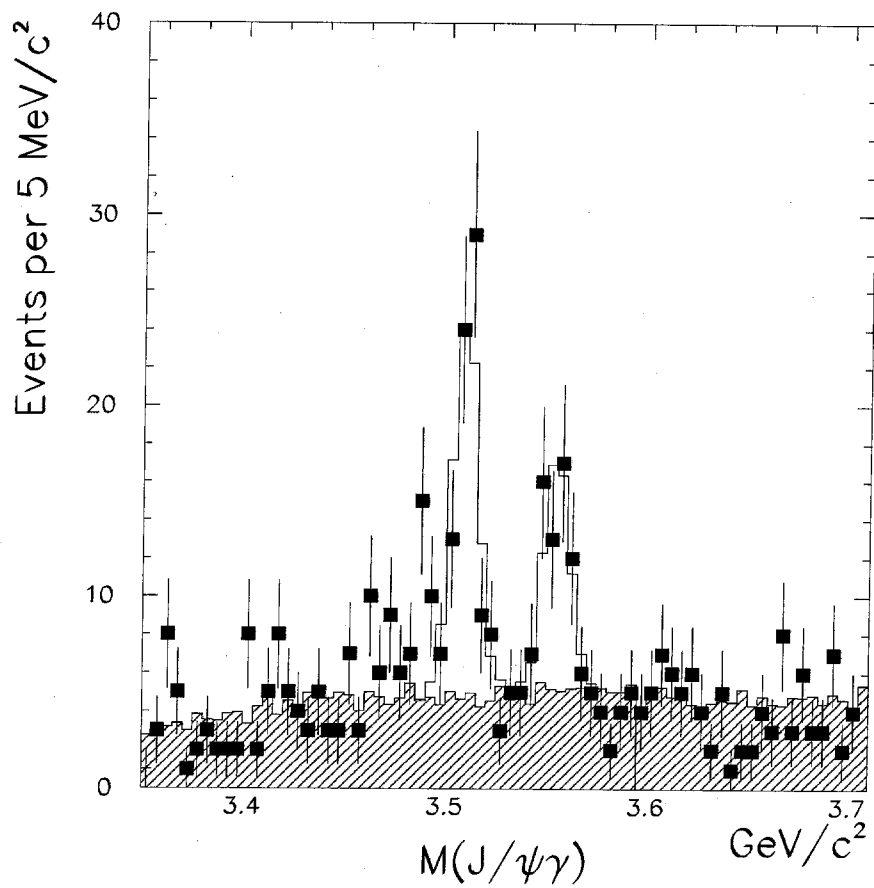


Figure 1: The $J/\psi\gamma$ mass spectrum. The background estimate is indicated by the shaded area, and the solid line histogram shows the result of the likelihood fit for the χ_{cJ} signals.

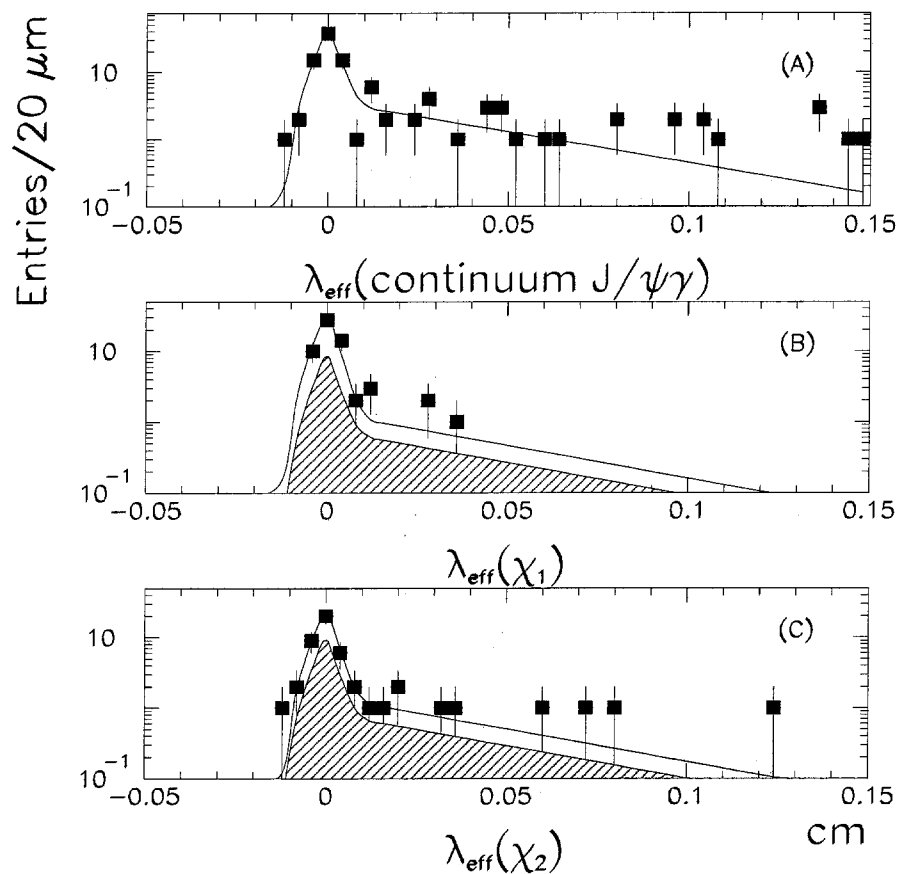


Figure 2: The $J/\psi\gamma$ effective decay length spectrum for events measured in the SVX. (A) The decay length distribution for candidates having $3350 \text{ Mev}/c^2 < M(J/\psi\gamma) < 3470 \text{ Mev}/c^2$ and $3590 \text{ Mev}/c^2 < M(J/\psi\gamma) < 3710 \text{ Mev}/c^2$. (B) The decay length distribution for the χ_{c1} , $3492 \text{ Mev}/c^2 < M(J/\psi\gamma) < 3528 \text{ Mev}/c^2$. (C) The decay length distribution for the χ_{c2} , $3538 \text{ Mev}/c^2 < M(J/\psi\gamma) < 3574 \text{ Mev}/c^2$. The fit to the data points is shown in each distribution. The shaded functions in (B,C) indicate the effective decay length distribution due to background sources.